International Forum on Aeroelasticity and Structural Dynamics
IFASD 2017
25-28 June 2017, Como - Italy

AEROSERVOELASTIC STABILITY ANALYSIS OF AN AIR-BREATHING HYPERSONIC VEHICLE

Huangda Zhao, Chao Yang, and Zhigang Wu

School of Aeronautic Science and Engineering, Beihang University
zhaohuangda@buaa.edu.cn

Keywords: ASE stability, Aerodynamic hearting, Unsteady thrust.

Abstract: With the development of aeronautics and astronautics, research on air-breathing hypersonic vehicles (AHV) has made many achievements. The latest hypersonic vehicles usually use the integrated body / engine configuration. The introduction of propulsion system brings a lot of new challenges to AHV. In this paper, the stability of the system is analyzed by using high efficiency engineering method, and the influence of the propulsion system and thermal effect on the system is discussed emphatically. Thermal analysis is performed by using layered solution method. Unsteady aerodynamic force is calculated by local piston theory. Steady and unsteady thrusts are both included in the stability calculation. The results show that the introduction of propulsion system results in a relative large decrease in the stability margin in this particular AHV. The effect of aerodynamic heating on system is mainly reflected in the decline of structural modal frequency, which makes the system tend to be unstable. The methods described above have little computational expense and acceptable accuracy, which can offer basic understanding of an AHV model in the preliminary design phase.

1 INTRODUCTION

Aeroservoelasticity(ASE) considers the interaction between aerodynamics, inertial, actuation, and control system. With the development of aeronautics and astronautics, research on air-breathing hypersonic vehicles (AHV) has made many achievements. The introduction of propulsion system brings a lot of new challenges to AHV[1]. Therefore, it is necessary to model and analyze the coupling between traditional ASE problem and the propulsion system.

Due to the high fight speed, aerodynamic heating phenomenon is very obvious during the flight of AHV[2]-[3]. In order to achieve long-range cruise distance, a high weight ratio of fuel to structure is required, which makes the overall stiffness of the vehicle smaller. On the other hand, for most metallic materials, modulus of elasticity decreases as the temperature increases, causing the rigidity of the structure decrease. Therefore, the design of modern hypersonic vehicle requires analysis of ASE problem in thermal environment.

In recent years, with the development of air-breathing hypersonic vehicle, the coupling between propulsion system, aerodynamics, structure, thermal effect, and control system has been paid more and more attention. In [4] , frequency domain analysis results of an AHFV were given. The calculations show that the thrust and engine inlet pressure are both affected by the pitch control surface (elevator) over a wide range of frequency. At the same time, changes in fuel flow rate and nozzle area can also affect the pitch angular velocity of an AHFV.

Rudd and Pines [5]studied the fight dynamic characteristics of a hypersonic waverider at Mach 10 , 30km. The finite element method was used for acquiring the aerodynamic pressure, and the drag force was calculated by using the reference temperature method. The results show that in order to establish the controller of the system, propulsion system must be accurately modeled.

Mirmirani etc. [6] believe that for air-breathing hypersonic vehicles, there is still no complete and accurate model to consider the characteristics of such aircrafts. In [6], a full-size hypersonic vehicle is studied using a high-precision CFD model. Firstly, a simple two-dimensional model is studied under the condition of Mach 10 and height of 30km. Then, based on the linear time-varying model [7], the control of the AHV model is discussed.

In the research of aerothermoelasticity, early studies included the effect of temperature in the static aeroelastic analysis of a double –wedge airfoil supported by a cantilever beam. Thermal stress is introduced from a parabolic distribution thermal field. The results show that thermal stress can affect torsional stiffness and cause stress stiffening phenomena [8]

Heeg[3] performed the aerothermoelasticity analysis of a NASP vehicle using Newton impact theory and piston theory. Surface temperature distribution was calculated by APAS software. Increasing the temperature reduced material properties, thus affecting the stiffness of the structure. It was found that the highest temperature appeared in the middle of the trajectory with a Mach number of 15 and a height of about 100,000 feet. Thermal effect caused the nature frequency of the structure decreased by about 30%. At normal temperature, the model did not flutter, but after applying thermal load the flutter occurred. Further analysis takes into account the effects of thermal stress, resulting in a natural frequency decrease of 13% -20% and a flutter boundary of about 25%.

The problem of Aerothermoelasticity at hypersonic flow is very complicated. According to the experience of research in NASP [9], the idea of layered solution method can be applied to the engineering analysis of hypersonic aerothermoelasticity. Because of the high efficiency of this method [10], it is used to analyze thermal mode in this paper.

This study is motivated by the need for a general understanding of thermal-structural-fluid-propulsive coupling of AHV in hypersonic flow. In order to provide some reference for the preliminary design stage of this kind of vehicle, a rapid analysis model is developed. The following two issues are mainly discussed: 1) the influence of the introduction of the propulsion system on the stability of the system 2) the analysis process of thermal effect and its influence.

2 MODELING METHODS

2.1 ASTEP problem analysis process

(Aeroservo-thermoelastic-propusive) ASTEP interactions include so many coupled subsystems that analyzing the whole coupled terms is very complicated and require huge computational costs. In order to obtain the general characters of an AHV in preliminary design phase, certain factors need to be decoupled or neglected. This section shows a relatively simple method to introduce propulsion system to the original aeroservoelastic problem.

The traditional aeroelastic solution equation is:

$$\mathbf{M}\ddot{\mathbf{q}} + \mathbf{C}\dot{\mathbf{q}} + \mathbf{K}\mathbf{q} = \mathbf{f} \tag{1}$$

Where M, C, K is the generalized mass matrices, generalized damping matrices, and generalized stiffness matrices, respectively. In order to model ASE system, it is necessary to define a variable which be connected with control system and form the coupling mechanism of mutual feedback. Under generalized coordinates, the degree of freedom of control surface is added into the system. Neglecting the inertia term of the rudder surface, Eq. (1) can be written as:

$$\begin{aligned}\mathbf{f} &= \mathbf{Q}_{\mathbf{q}} + \mathbf{Q}_{\delta} \\ &= \frac{1}{2}\rho V^2 \mathbf{A}_{q0}\mathbf{q} + \frac{1}{2}\rho V \mathbf{A}_{q1}\dot{\mathbf{q}} + \frac{1}{2}\rho V^2 \mathbf{A}_{\delta 0}\delta + \frac{1}{2}\rho V \mathbf{A}_{\delta 1}\dot{\delta}\end{aligned} \tag{2}$$

In order to introduce the propulsion system, based on the traditional ASE stability analysis, the engine inlet conditions and the generated thrusts is added. Figure 1 shows the analysis framework used in this study.

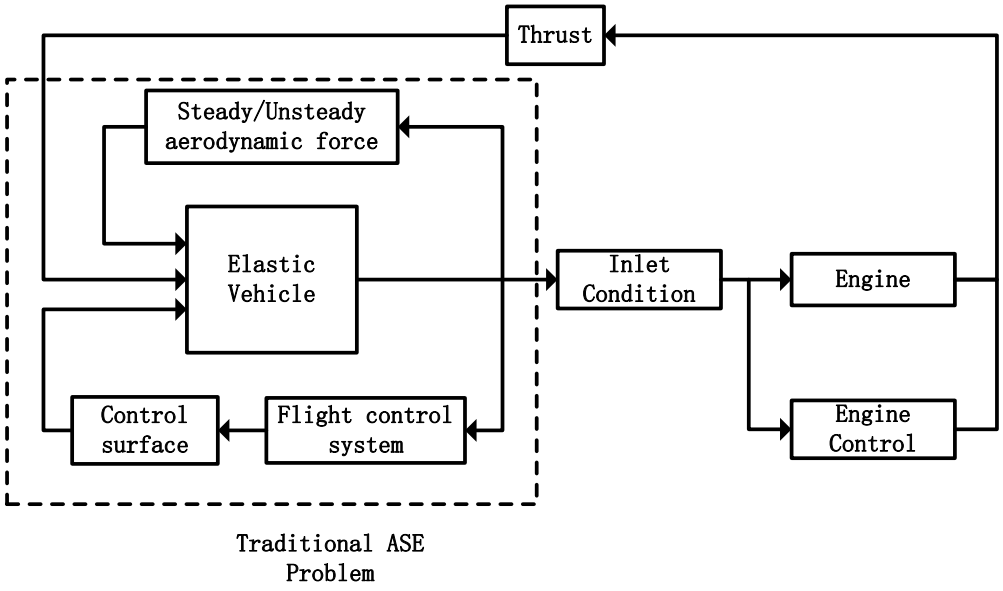

Figure 1: Aeroservo-thermoelastic-propusive interactions analysis framework

Method that can model the propulsion system and calculate the thrust is not the focus of this study. Engine thrust is treated as known data, which is given in the form:

$$\mathbf{T} = \mathbf{T}_x + \mathbf{T}_y + \mathbf{T}_z = \frac{1}{2}\rho V^2 c_x S_p + \frac{1}{2}\rho V^2 c_y S_p + \frac{1}{2}\rho V^2 c_z S_p \tag{3}$$

Where $\mathbf{T}_x$, $\mathbf{T}_y$ and $\mathbf{T}_z$ are the components of the total force generated by engine in three directions. For the analysis of longitudinal direction problems, it can be considered that the lateral force $\mathbf{T}_y$ is zero. S_p is the reference area of the engine and c is a function of engine

inlet parameter. Angel of attack is used here because it is convenient to be added to the system. Similarly, **T** can be written in the form of generalized aerodynamic forces as:

$$\begin{aligned}\mathbf{Q}_{\mathrm{T}} &= \phi_{tp,x}^{T}\frac{\partial \mathrm{T}_x}{\partial\alpha}\alpha+\phi_{tp,z}^{T}\frac{\partial \mathrm{T}_z}{\partial\alpha}\alpha \\ &= \phi_{tp,x}^{T}\frac{\partial \mathrm{T}_x}{\partial\alpha}\phi_{inlet,\alpha}\mathbf{q}+\phi_{tp,z}^{T}\frac{\partial \mathrm{T}_z}{\partial\alpha}\phi_{inlet,\alpha}\mathbf{q} \\ &= \phi_{tp,x}^{T}\frac{1}{2}\rho V^2 c_{x\_\alpha}S_p\phi_{inlet,\alpha}\mathbf{q}+\phi_{tp,z}^{T}\frac{1}{2}\rho V^2 c_{z\_\alpha}S_p\phi_{inlet,\alpha}\mathbf{q} \\ &= \frac{1}{2}\rho V^2\mathbf{A}_{Tx}\mathbf{q}+\frac{1}{2}\rho V^2\mathbf{A}_{Tz}\mathbf{q}\end{aligned} \tag{4}$$

As can be seen from Eq. (4), the unsteady force caused by the propulsion system includes two terms, one is the unsteady thrust in the axial direction and the other is the unsteady lift. The solution equation then can be written as:

$$\mathbf{M}\ddot{\mathbf{q}}+\mathbf{C}\dot{\mathbf{q}}+\mathbf{K}\mathbf{q}=\frac{1}{2}\rho V^2\mathbf{A}_{q0}\mathbf{q}+\frac{1}{2}\rho V\mathbf{A}_{q1}\dot{\mathbf{q}}+\frac{1}{2}\rho V^2\mathbf{A}_{\delta 0}\delta+\frac{1}{2}\rho V\mathbf{A}_{\delta 1}\dot{\delta}+\frac{1}{2}\rho V^2\mathbf{A}_{Tx}\mathbf{q}+\frac{1}{2}\rho V^2\mathbf{A}_{Tz}\mathbf{q} \tag{5}$$

Eq. (5) can be easily transformed into frequency domain, and calculate the transfer function. After modeling control system and other subsystems, the system's open-loop transfer function can be obtained. Finally, the stability equation is solved by using the Nyquist stability criterion. The specific method can be found in the related literature [11].

2.2 Aerothermoelastic problem Analysis Process

In this study, thermal analysis is carried out by using the layered solution method. The basic assumption of this method is that the unsteady aerodynamics do not contribute to the aerodynamic heating, and the unsteady aerodynamic force is not affected by the aerodynamic heat, but only effected by the structural dynamic characteristics. The main advantages include: 1) The coupling mechanism is easy to be understand and implement by engineering code, 2) Method has an acceptable accuracy, which can meet most engineering needs, 3) Calculation expense is little and can be used the concept and initial design phase.

Figure 2 shows the analysis framework of the layered solution method. In this analysis process, constant aerodynamic force is the initial input to the system. For complex vehicle shapes, CFD technology can effectively capture the flow characteristics. Taking into account the computational efficiency and accuracy, the steady Euler method is used to calculate the static pressure distribution. The flow parameters are obtained based on the commercial software FLUENT, and the heat flux is calculated by the reference temperature method. The unsteady aerodynamic force is generated by using the thermal modal shape and the local flow parameters, and be used in the stability analysis of the whole system.

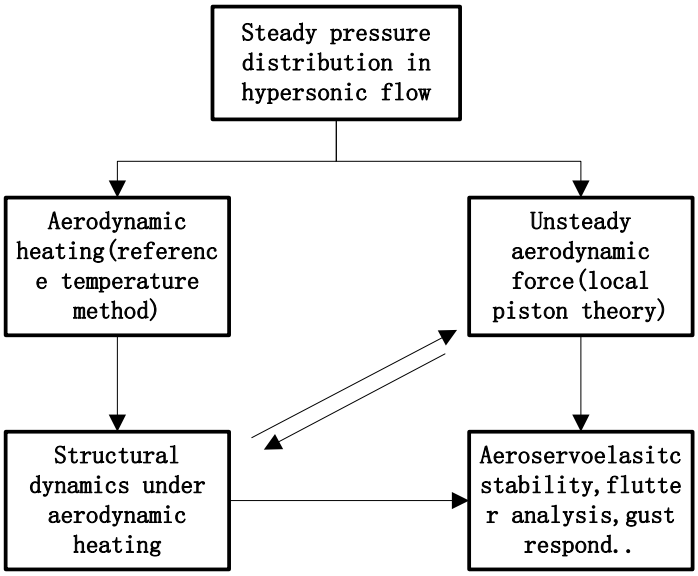

Figure 2: Aerothermoelastic problem analysis framework

2.3 Aerodynamic Pressure

Piston theory is an efficient engineering method, which can get accurate estimation of the unsteady aerodynamic force. In order to capture the flow characteristics of a complex shape, CDF method can be introduced to calculate the flow field parameters. Local piston theory is a continent way to combine unsteady effect with flow characteristics.

The basic assumption of Pistons theory is that the thickness of the wing profile is very thin and the Mach number is high. Under these assumptions, the perturbation of a point on the surface of a vehicle has little effect on other points. Piston theory omitted this effect, and considers that aerodynamic pressure at a certain point can only be affected by its wash velocity. It is clear that Piston theory does not take into account the three-dimensional effect, but in fact this effect is relatively low in the high Mach number domain [11].

The expression of the piston theory is:

$$P = P_{\infty}\left(1+\frac{\gamma-1}{2}\frac{W}{c_{\infty}}\right)^{\frac{2\gamma}{\gamma-1}} \tag{6}$$

When a strong three-dimensional effect is encountered, or the surface angle is large, the surface airflow parameters calculated by the steady flow can be used to replace the free flow parameters in piston theory, which is the basic treatment of local piston theory. By performing Taylor expansion of Eq. (6), and using local flow parameters, pressure coefficient can be written as [12]:

$$C_p(x,t)=\frac{2}{Ma_{local}^2}\left[\frac{v_n}{a_{local}}+\frac{(\gamma+1)}{4}\left(\frac{v_n}{a_{local}}\right)^2+\frac{(\gamma+1)}{12}\left(\frac{v_n}{a_{local}}\right)^3\right]$$
$$v_n=\frac{\partial Z(x,t)}{\partial t}+V_{local}\left\{\frac{\partial Z(x,t)}{\partial x}\right\} \tag{7}$$
$$Z(x,t)=w_d(x,t)$$

2.4 Aerodynamic Hearing

The aerodynamic heating is calculated using the extensively used Eckert reference temperature method [13]. The principle of the reference temperature method is that: when the air flow passes through the plate, if the temperature T and the temperature-related term of the plate are corrected (reference temperature), so that the shear stress calculated by the reference parameters in incompressible flow is exactly equal to the shear stress in compressible flow, then a reference temperature can be used to replace the original stable temperature. In this condition, compressible flow can be calculated using incompressible friction formula [14] . The reference temperature can be acquired by:

$$T^*=0.5T_w+0.22T_r+0.28T_e \tag{8}$$

After obtaining the reference temperature, the temperature-dependent parameters in the incompressible flow must be determined using the reference temperature. The reference density and the reference viscosity coefficient can be determined by the equation of state and the Salentian formula:

$$\rho^*=\frac{p_e}{RT^*}$$
$$\mu^*=\left(\frac{T^*}{288.15}\right)^{1.5}\frac{398.55}{T^*+110.4}\times 1.7894E-5 \tag{9}$$

The relationship between the coefficient of friction and Reynolds number under turbulence conditions is Eq. (10), and after a series of derivation, the thermal flux into the structure is determined by Eq. (11)

$$C_f^*=\frac{0.37}{\left(\log_{10}\mathrm{Re}_x^*\right)^{2.584}} \tag{10}$$

$$St=\frac{C_f^*}{2\,\mathrm{Pr}^{2/3}}$$
$$Q_{aero}=\rho_e u_e c_p\left(T_r-T_w\right)St^* \tag{11}$$
$$Q_{rad}=\sigma\varepsilon\left(T_w^4-T_\infty^4\right)$$
$$Q=Q_{aero}-Q_{rad}$$

3 RESULT AND DISSCUSSION

3.1 Example model description

The model studied in this paper is an air-breathing hypersonic vehicle. The shape of this vehicle is shown in Figure 3. The model has a total length of 4.8m and total mass of 1500kg.This kind of vehicle usually needs to climb to a certain height through other aircraft or booster, and reach the working speed of the scramjet engine. When analyzing the coupling effect of the propulsion system, the flying trajectory marked in Figure 4, during which the scramjet is opened, is selected as the analysis area.

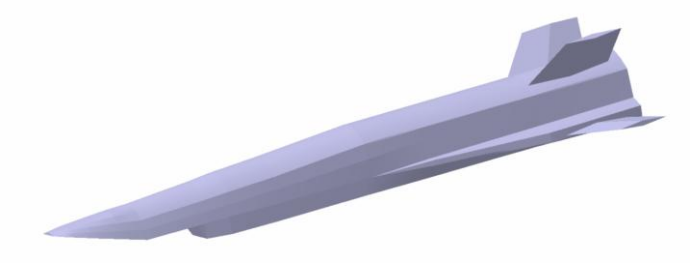

Figure 3: Air-breathing hypersonic vehicle model used in this study

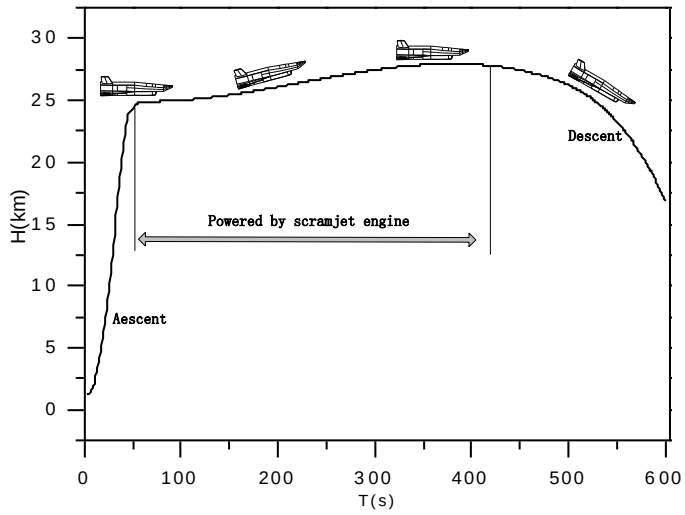

Figure 4: Flying trajectory and analysis area

Table 1 listed four important analysis states selected in the trajectory. Subsequent work will be based on these four status points.

Status	Height/km	Mach number	AOA/ °
1	25.0	6.0	0.0
2	25.1	6.0	5.0
3	25.3	6.0	0.0
4	28.0	6.5	0.0

Table 1: Analysis status selected

3.2 Aerodynamic characteristics

Since the analysis is based on the CFD calculation results, the aerodynamic characteristics of the model are given firstly. The commercial software ANSYS.FLUENT is used to calculate the unstructured aero boxes. The total number of element and grid are 79872 and 434969 respectively. Far - field boundary conditions are implemented. The element distribution is shown in Figure 5, and the pressure distribution on the surface of the aircraft is shown in Figure 6. The main mechanical properties are shown in table 2.

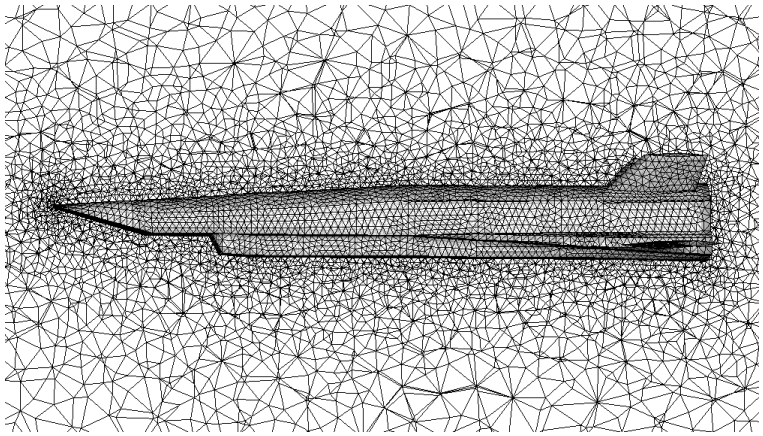

Figure 5: Element distribution illustration

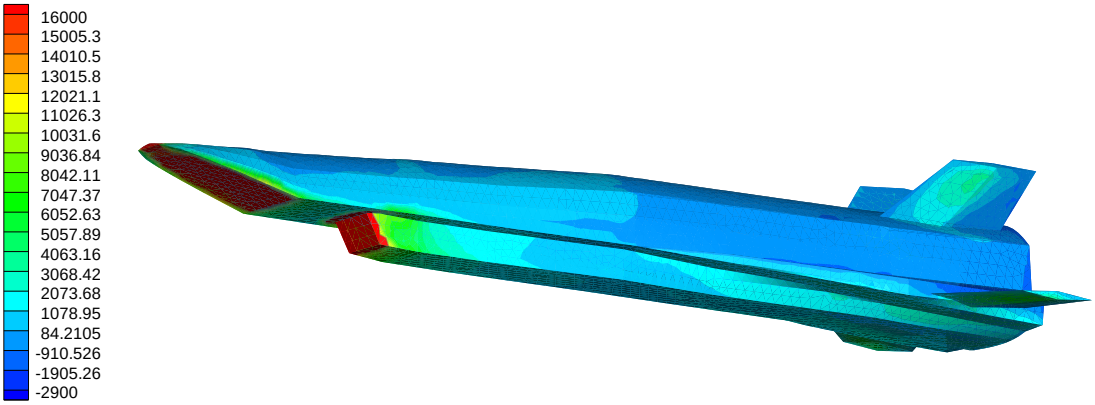

Figure 6: Pressure distribution at Mach 6 and 5 deg angel of attack

Status	Altitude /km	Atmospheric Pressure /Pa	Density kg/m3	AOA/ °	Lift coefficient
1	25.0	2549.2	0.0400	0.0	5.88e-3
2	25.1	2510.5	0.0394	5.0	2.33e-2
3	25.3	2434.9	0.0312	0.0	5.90e-3
4	28.0	1616.2	0.0205	0.0	6.08e-3
Reference area		10 m^2	Reference length		5m

Table 2: Aerodynamic characteristics of an AHV

In the calculation of unsteady aerodynamics, it is necessary to redraw the aerodynamic boxes suitable for piston theory. Modal shape (thermal modal shape or non-heated modal shape) is also needed. The first two longitudinal bending modes are showed in Figure 7.

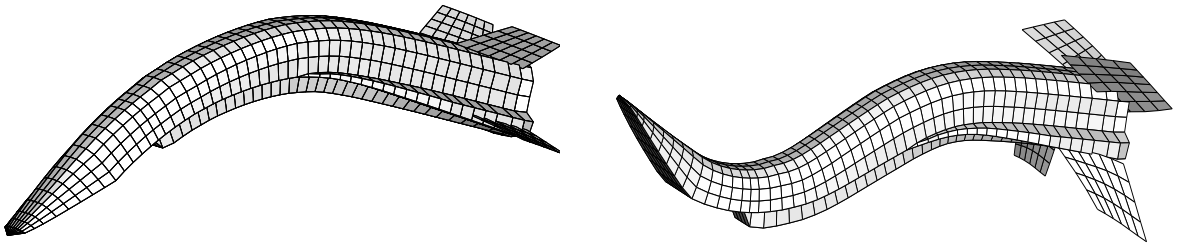

Figure 7: First two longitudinal bending modes

3.3 Structural dynamic characteristics

Performing Aeroservoelasticity analysis requires the structural modal shape and elastic natural frequency, which is provided by analyzing the finite element model. The method of modal analysis is relatively mature. Under the unheated condition, the first five natural frequencies of the AHV are shown in table 3.

Status	1st Vertical bending/HZ	1st Lateral bending/HZ	2nd Vertical bending/HZ	2nd Lateral bending/HZ	1st Torsion /HZ
1	25.17	22.83	50.53	50.19	52.72
2	25.19	22.86	50.54	50.20	52.73
3	26.26	24.10	50.71	50.22	52.81
4	27.78	25.92	50.87	50.23	52.85

Table 3: Structural dynamic characteristics of an AHV

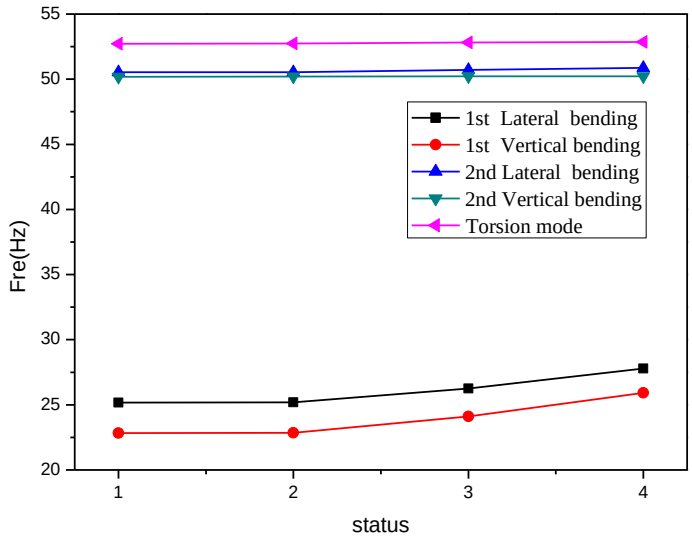

Figure 8: Structural dynamic characteristics of an AHV

The modal shapes of the finite element model are similar to those in Figure 7 . It can be seen from Figure 8 that the frequency of each status is slightly increasing, which is mainly due to the decrease of total mass due to the consumption of fuel. The overall difference is not big.

3.4 System stability analysis

In this section, we mainly discuss the effect of the propulsion system on the longitudinal stability of the aircraft. The 1st longitudinal bending and the 2nd longitudinal modes are selected in the analysis, together with two rigid body mode and one control surface mode. The single-input single-output (SISO) Nyquist stability method is used to obtain the stability margin.

First, the stability margin under standard condition (regardless of the propulsion system coupling and aerodynamic heating) is given in table 4

Status	Nyquist amplitude margin/db	Nyquist phase margin/deg	Amplitude margin at 1st bending fre/db	Amplitude margin at 2nd bending fre/db
1	19.20	63.84	8.06	40.51
2	17.31	66.48	6.26	38.80
3	23.87	69.67	12.55	46.91
4	19.67	65.53	7.98	43.79

Table 4: Stability margin of the system under standard condition

The amplitude margin and phase margin of each state satisfy the stability requirement. The Nyquist margin of the rigid body is large and it is not easy to be unstable. It is necessary to pay attention to the stability margin at elastic bending frequencies. Under certain conditions, perturbations (such as propulsion system or aerodynamic heating) may cause a lack of stability margin.

3.4.1 Effect of prolusion system on system stability characteristics

From the calculation and analysis above, it can be seen that state 2 is the most dangerous point so that the propulsion-coupling stability analysis is carried out in this particular state. It should be noted that, the engine module is treated as a black box. There is no relevant engine modeling and calculation, therefore, the pressure redistribution caused by the engine thrust cannot be obtained. But the steady thrust is of the same order of total lift of the aircraft, thus cannot be neglected. Therefore, in order to explain the problem in a better way, the effect of constant thrust is estimated by a coefficient-correction. Such approach may be inaccurate due to the constraints of the input data, but the effect of constant thrust can be estimated in a certain degree.

By using the total lift in trimmed state as a reference value, it is assumed that the pressure change due to the ignition of the engine can affect the whole aircraft surface (not only the lower rear surface of the vehicle), and letting $\mathbf{c}_z = (\mathbf{T}_z + \mathrm{L})/\mathrm{L} \cdot \mathbf{c}_z$ Can be used to correct the real part of the generalized aerodynamic influence coefficient matrix and is given 1.325 in this particular status. The result is shown in table 5.

Status 2	Nyquist amplitude margin/db	Change db(%)	Amplitude margin at 1st bending fre/db	Change db(%)
NT	17.31	-	6.26	-
UT	17.15	0.16(0.92%)	6.14	0.12(1.92%)
ST	14.95	2.36(13.63%)	3.83	2.43(38.82%)
NT&ST	14.78	2.53(14.62%)	3.77	2.49(39.78%)
TE& NT&ST	13.29	4.02(23.22%)	2.71	3.55(56.71%)
Note : NT -without thrust ,UT-with unsteady thrust ,ST-with steady thrust, TE-with thermal effect				

Table 5: Stability margin of the status 2 with/without steady/unsteady thrust

The analysis shows that for this particular AHV, the addition of unsteady thrust has little effect on the stability of the system. The effect of constant thrust on the stability is significant, which is mainly related to the lift generated by propulsion system in the calculation. In the state 2, the coefficient $\mathbf{c}_z$ is relatively large, thus causing quite reduction of stability margin. More accurate analysis should recalculate the pressure distribution under engine operating conditions. Including both steady and unsteady thrust, the stability margin of the system decreases more, this is reasonable in this model.

Here, an analysis is done including both thermal effect and the propulsion system. The the effects of heat will be discussed in next section. The Nyquist curve and the bode curve are shown in Figure 9 and Figure 10.

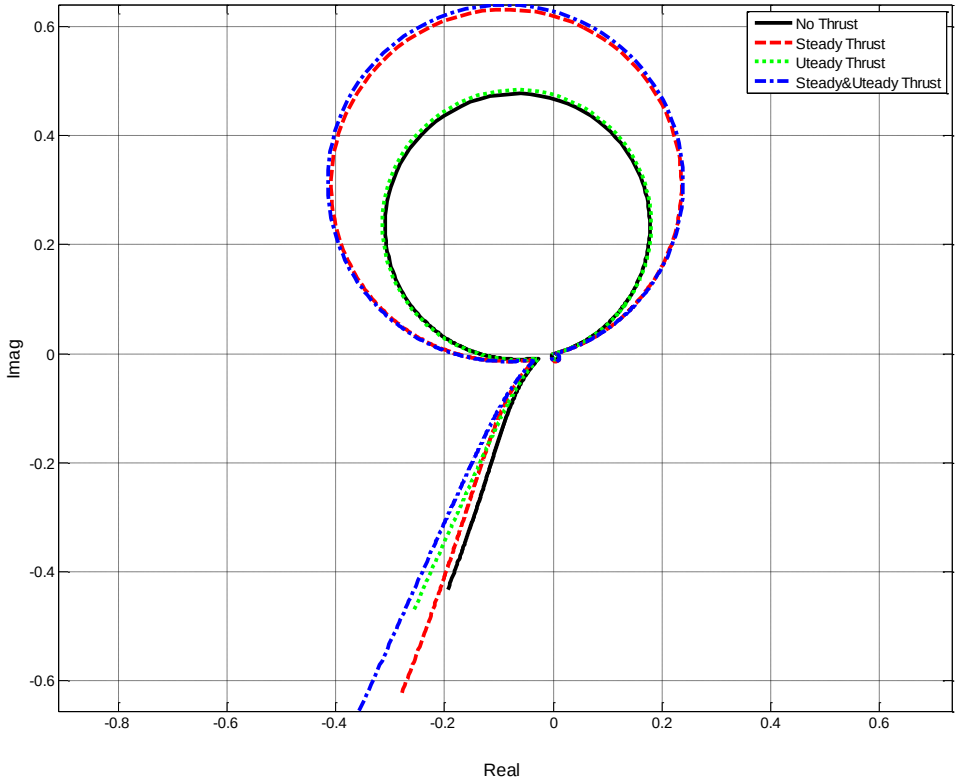

Figure 9: Nyquist curve of the system at status 2

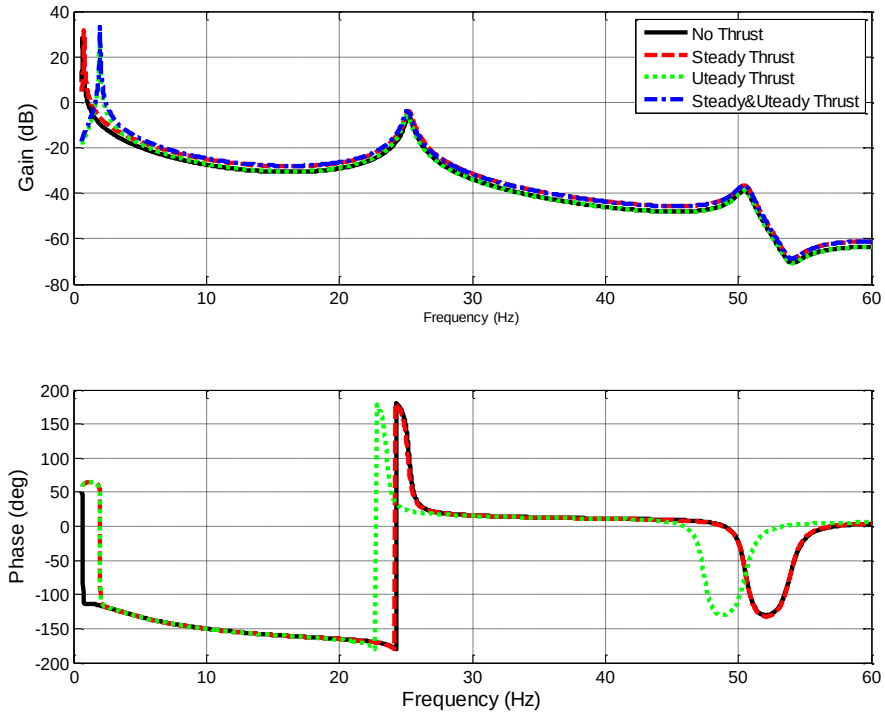

Figure 10: Bode curve of the system at status 2

3.4.2 Effect of aerodynamic heating on system stability characteristics

Since layered solution method is a one-way coupled method, the effect of aerodynamic heating on system stability is mainly caused by changing the elastic frequency of the structure. Here, the frequency variation of the first 2 longitudinal modes of each status is given in table 6.

Status	1st Vertical bending/HZ	Heated state	2nd Vertical bending/HZ	Heated state
1	25.17	23.59	50.53	47.37
2	25.19	23.61	50.54	47.38
3	26.26	24.62	50.71	47.54
4	27.78	26.04	50.87	47.69

Table 6: Structural dynamic characteristics of an AHV in heated state

The structural temperature field of the status 2 is shown in Figure 11, the high temperature domain occurs at the lower surface of this AHV.

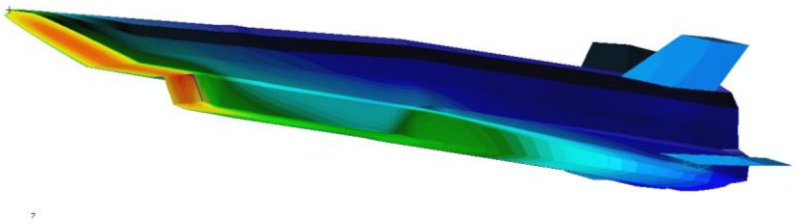

Figure 11: Air-breathing hypersonic vehicle model used in this study

By comparing with the frequency at normal temperature, it can be found that the modal frequencies of the structures in heated state are decreased. Part of the reason is that the elastic modulus of the material decreases with increasing temperature, so the stiffness of the structure decreases, resulting in a decrease in the modal frequency. The stability margin of the system under thermal conditions (without thrust) is listed in table 7.

Status	Nyquist amplitude margin/db	Nyquist phase margin/deg	Amplitude margin at 1st bending fre/db	Amplitude margin at 2nd bending fre/db
1	19.20	63.84	8.06	40.51
1H	17.74	61.81	7.02	39.48
rate	7.71%	3.18%	12.9%	2.54%
2	17.31	66.48	6.26	38.80
2H	15.84	66.48	5.21	37.77
rate	8.49%	0.00%	16.77%	2.65%
3	23.87	69.67	12.55	46.91
3H	22.39	69.66	11.49	45.88

rate	6.20%	0.014%	8.45%	2.20%
4	19.67	65.53	7.98	43.79
4H	18.20	65.53	6.91	42.78
rate	7.47%	0.00%	13.41%	2.31%

Table 7: Stability margin of the system under thermal conditions

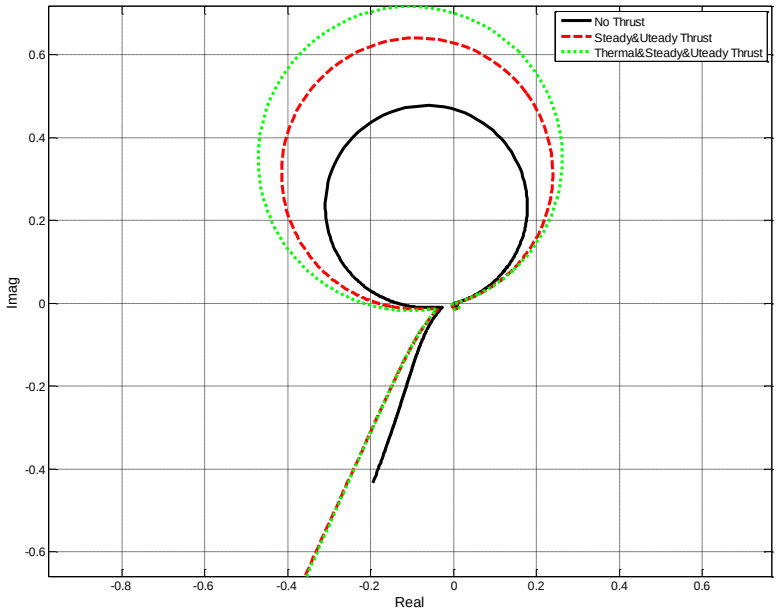

Figure 12: Nyquist curve of the system at status 2

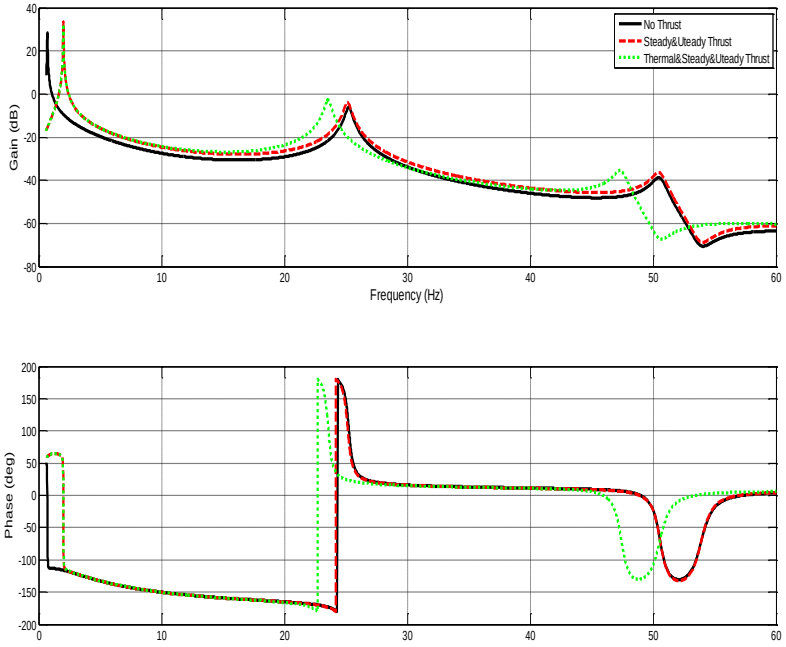

Figure 13: Bode curve of the system at status 2

Similar to the propulsion system, the aerodynamic heating effect also reduces the stability of the system. For status 2, if both propulsion system and the thermal effect are considered, the system is in the most dangerous situation. Attentions should be paid at this situation, which the system may need to be improved or redesigned. Nyquist and bode curve can be seen in Figure 12 and Figure 13.

4 CONCLUSION

A comprehensive ASTEP model is developed for analysis of air-breathing hypersonic vehicles. Engineering methods are used to perform fast analysis in preliminary design phase. Propulsion system and aerodynamic heating effect is added to the traditional ASE analysis process. The results of these studies allow one to reach several useful conclusions:

(1)For the model studied in this paper, unsteady thrust has little effect on system stability while the effect of constant thrust on the stability is significant. Propulsion system may cause the system unstable, and should not be neglected.

(2)The effect of aerodynamic heating on system stability is mainly caused by changing the elastic frequency of the structure. Similar to the propulsion system, the aerodynamic heating effect also reduces the stability of the system.

(3) Propulsion system can cause a significant change in the pressure distribution and it is recommended that engine model be built in further analysis.

5 REFERENCES

[1] Chavez, F. R., and Schmidt, D. K., “Analytical Aeropropulsive/Aeroelastic Hypersonic-Vehicle Model with Dynamic Analysis,”Journal of Guidance, Control, and Dynamics, Vol. 17, No. 6, Nov.–Dec. 1994, pp. 1308–1319.

[2] Bertin J J. Hypersonic aerothermodynamics[M]. Aiaa, 1994.

[3] Heeg J, Zeiler T A, Pototzky A S, et al. Aerothermoelastic analysis of a NASP demonstrator model[C]//AIAA/ASME/ASCE/AHS/ASC 34th Structures, Structural Dynamics, and Materials Conference. 1993, 1: 617-627.

[4] Schmidt, D. K., Mamich, H., and Chavez, F., “Dynamics and control of hypersonic vehicles, The integration challenge for the 1990s,” AIAA Paper 91-5057, Dec. 1991.

[5] Rudd, Lael, and Pines, Darryl, “Integrated Propulsion Effects on Dynamic Stability and Control of Hypersonic Waveriders,”AIAA Paper 2000-3826, July 2000.

[6] Mirmirani, M., Wu, C., Clark, A., Choi, S., and Colgren, R., “Modeling for Control of a Generic Air-Breathing Hypersonic Vehicle,”AIAA Paper 2005-6256, Aug. 2005.

[7] Fidan, B., Kuipers, M., Iannou, P., and Mirmirani, M.,“Longitudinal Motion Control of Air-Breathing Hypersonic Vehicles Based on TimeVarying Models,”AIAA Paper 2006-8074, Nov. 2006

[8] Biot M A. Influence of Thermal Stresses on the Aeroelastic Stability of Supersonic Wings[J]. Journal of the Aeronautical Sciences, 1957, 24(6): 418-420.

[9] Spain C V, Soistmann D L, Parker E C, et al. An overview of selected NASP aeroelastic

studies at the NASA Langley Research Center[C]//AIAA, Aerospace Sciences Meeting. 1990, 1.

[10] Zhigang, Hui Junpeng, Yang chao. "Hypersonic aerothermoelastic analysis" Journal of Beijing University of Aeronautics and Astronsutics, 2005, 32 (3): 270-273

[11] Yang chao,Wu zhigan,Wan zhiqiang. Aeroelastic Principle of Aircraft [M].Beihang university Press,2011

[12] McNamara, J. J., Crowell, A. R., Friedmann, P. P., Glaz, B., and Gogulapati, A., Approximate Modeling of Unsteady Aerodynamics for Hypersonic Aeroelasticity[J], Journal of Aircraft, 2010, 47(6): 1932–1945.

[13] Qian Yiji. Aerodynamics [M]. Beijing University of Aeronautics and Astronautics Press, 2004.

[14] Spain C V, Zeiler T A, Gibbons M D, et al. Aeroelastic character of a national aerospace plane demonstrator concept[C]//AIAA/ASME/ASCE/AHS/ASC 34th Structures, Structural Dynamics, and Materials Conference. 1993, 1: 163-170.

COPYRIGHT STATEMENT